Chinese Chemical Letters 35 (2024) 108931

Contents lists available at ScienceDirect

Chinese Chemical Letters

journal homepage: www.elsevier.com/locate/cclet

The new challenges for the development of NH_3-SCR catalysts under new situation of energy transition in power generation industry

Feibin Wei[a], Yongfang Rao[e], Yu Huang[b,c,*], Wei Wang[b,c,d], Hui Mei[a,**]

[a] Science and Technology on Thermostructural Composite Materials Laboratory, School of Materials Science and Engineering, Northwestern Polytechnical University, Xi'an 710072, China
[b] Key Laboratory of Aerosol Chemistry and Physics, State Key Laboratory of Loess and Quaternary Geology (SKLLQG), Institute of Earth Environment, Chinese Academy of Sciences, Xi'an 710061, China
[c] Center of Excellence in Quaternary Science and Global Change, Chinese Academy of Sciences, Xi'an 710061, China
[d] University of Chinese Academy of Sciences, Beijing 100049, China
[e] Department of Environmental Science and Engineering, Xi'an Jiaotong University, Xi'an 710049, China

ARTICLE INFO

Article history:
Received 25 April 2023
Revised 23 July 2023
Accepted 13 August 2023
Available online 15 August 2023

Keywords:
NH_3-SCR
NOx reduction
Power generation
Ultra-low temperature
Wide temperature windows

ABSTRACT

NH_3-SCR was one of the most promising deNO_x technologies and it has been widely applied in industrial NO_x reduction. However, with the further development of energy transformation in power generation sector, the development of NH_3-SCR catalysts is facing some new challenges. It is becoming an urgent problem to solve low catalytic activity and stability of NH_3-SCR catalysts at the working condition of ultra-low temperature ($\leq$ 200 °C) and high concentrations of H_2O+SO_2 due to the gradual deployment of new energy power plants. Furthermore, the traditional coal-fired power plants would need flexible operation with the increasing share of renewable energy generation. The NH_3-SCR catalysts which were applied in coal-fired power industry would be requested to work in a wide temperature window from 200 °C to 500 °C in the near future. Therefore, in this review, we summarized the progress of NH_3-SCR catalysts in solving these different industrial problems in recent years. And the research directions which were deserved to be focused on the development of NH_3-SCR catalysts for the energy transition of power generation sector are proposed.

1. Introduction

Nitrogen oxides (NO_x), as one of the main air pollutants, could cause some serious environmental problems such as acid rain, photochemical smog [1–3]. Furthermore, some researchers found that the nitrogen oxides could also damage people's lungs and contribute to severe lung disease in recent years [4–6]. Therefore, how to reduce the concentration of NO_x in the air is important for the treatment of air pollution. The industrial production was one of the main sources of NO_x in the air. According to the statistics [7–9], the industrial NO_x mainly comes from the flue gas of some industrial sectors which use fossil fuels and nitric acids (*e.g.*, coal-fired power plants, municipal waste incineration, cement plants, steel plants). Therefore, in most countries of the world, the emission standard of NO_x in these industrial sectors was very strict (*e.g.*, coal-fired power plants: USA: 135 mg/m^3, EU: 200 mg/m^3, China: 100 mg/m^3) [10]. In order to meet the increasingly stringent emission standards of industrial NO_x, a lot of technologies have been applied to reduce the concentration of NO_x in flue gas from the industrial production. The general strategies for controlling NO_x emissions include selective non-catalytic reduction (SNCR), selective catalytic reaction (SCR), wet scrubbing, adsorption, electrochemical method and so on [11–16]. Among them, NH_3-SCR is becoming the most widely applied technology of NO_x removal in some industrial sectors due to its high efficiency and simplified operational procedure [17–20]. Generally, the main deNO_x reactions in NH_3-SCR are shown below (Eqs. 1–5) [21–23]:

$$4NH_3 + 4NO + O_2 \rightarrow 4N_2 + 6H_2O \text{ (Standard SCR)} \quad (1)$$

$$4NH_3 + 2NO + 2NO_2 \rightarrow 4N_2 + 6H_2O \text{ (“Fast”SCR)} \quad (2)$$

$$4NH_3 + 2NO_2 + O_2 \rightarrow 3N_2 + 6H_2O \quad (3)$$

* Corresponding author at: Key Laboratory of Aerosol Chemistry and Physics, State Key Laboratory of Loess and Quaternary Geology (SKLLQG), Institute of Earth Environment, Chinese Academy of Sciences, Xi'an 710061, China.
** Corresponding author.
E-mail addresses: huangyu@ieecas.cn (Y. Huang), meihui@nwpu.edu.cn (H. Mei).

https://doi.org/10.1016/j.cclet.2023.108931
1001-8417/

Table 1
The summary for composition and temperature of the flue gas in different industries.

Industries	Temperature of reaction (°C)	NO_x (mg/m^3)	SO_2 (mg/m^3)	Fly ash (mg/m^3)	Other compositions	Types of catalysts		Challenges
						Commercial	Un-commercial	
Coal-fired power	300–400	100–1000	500–4000	30–100	Heavy metals (Hg, Pb *etc.*)	V_2O_5-WO_3/TiO_2	Fe/Mn/Ce oxide catalysts; zeolite catalysts	SO_2 and Hg resistance, wide operating temperature window
Municipal waste incineration power	150–180	400–1000	200–1200	1000–10,000	Mg, K, Na, Ca, P, HCl			Low-temperature, SO_2, H_2O, alkali and alkaline earth metals resistance
Steel	80–200	200–310	400–1500	30–80	TCDD, CO, heavy metals *etc.*			Low-temperature, SO_2 and H_2O resistance
Cement	120–180	800–1200	30–100	80,000–120,000	CaO, HF *etc.*			Low-temperature, fly ash tolerance (abrasive resistance)
Coking	180–280	100–1200	100–5000	50–85	H_2S, CO, CO_2 *etc.*			Low-temperature
Glass	180–220	300–1400	300–3300	300–1200	HCl, HF, Na *etc.*			
Ceramics	80–150	200–1100	500–3500	50–200	HCl, Pb, Cd *etc.*			

$$4NH_3 + 6NO \rightarrow 5N_2 + 6H_2O \quad (4)$$

$$8NH_3 + 6NO_2 \rightarrow 7N_2 + 12H_2O \quad (5)$$

The general definition about NH_3-SCR reactions is "Standard SCR" or "Fast SCR". And the fast SCR is completed more quickly than standard SCR when the molar ratio of NO/NO_2 is 1:1 [24].

For NH_3-SCR technology, the development of low-cost and high-performance SCR catalysts is the key to achieve highly efficient removal of NO_x. In the past few decades, V_2O_5–WO_3/TiO_2 catalysts have been widely used in industrial deNO_x on account of its high efficiency in the temperature window of 300–400 °C [25–30]. However, with the expanding of the application scenarios of NH_3-SCR, the traditional V_2O_5–WO_3/TiO_2 catalysts are unable to meet the need of NH_3-SCR under different working conditions in different industries. As shown in Table 1, we summarized and compared the main characteristics of the flue gas in several typical industries.

According to this, the central challenges for the development of NH_3-SCR catalysts in different industries were proposed. And compared with other industries, the NH_3-SCR technology is facing some new challenges which are deserved to be discussed carefully in energy generation industry due to the deep transformations of energy sector. Specifically, with the prosperous development of new energy generation sector, the technology of electricity generation is going through a transition from traditional coal-fired to new energy power generation [31]. And the traditional power plants would account for decreasing percentage of the total electricity generating capacity in the near future. The coal-fired power plants would operate under a low-load condition for a long time. Therefore, the temperature of flue gas exhausted from coal-fired boiler would drop to about 200 °C. The activity of V_2O_5–WO_3/TiO_2 rapidly declines when the working temperature is below 300 °C or above 400 °C. Thus, the catalytic activity of V_2O_5–WO_3/TiO_2 can not meet the demand of deNO_x efficiency with the temperature below 300 °C. Therefore, how to develop novel SCR catalysts which could maintain high deNO_x efficiency in a wide temperature window from 200 °C to 400 °C is an urgent demand for the further application of NH_3-SCR technology in coal-fired power industry.

In addition, SO_2 poisoning for NH_3-SCR catalysts is another well-explored issue [32–35]. And it was generally accepted that the poisoning mechanism was the deposition of NH_4HSO_4 (ABS) and the sulfation of metal active sites [36]. As is reported, the deposition amount of ABS on catalyst surface would dramatically increase when the reaction temperature dropped to below 300 °C [32,37].

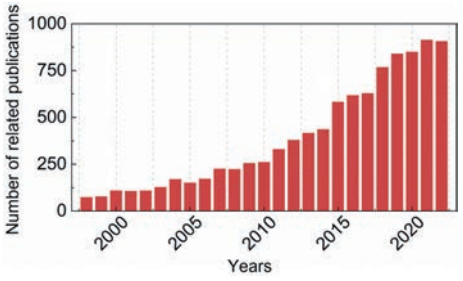

Fig. 1. Statistical data of articles on the topic of "SCR catalyst" published in the recent twenty five years. The data were compiled from the database of Web of Science Core Collection on May 18, 2023.

Therefore, another challenge for the development of NH_3-SCR catalysts in coal-fired power industry was how to improve SO_2 resistance of NH_3-SCR catalysts under low working temperature.

On the other hand, on account of the non-renewability of coals, people are trying to use renewable biomass energy to replace it as the main fuel to generate electricity. Thus, the technology of NH_3-SCR is facing an entirely different condition in new energy generation industry. In recent years, people come to recognize that municipal wastes could be used as a renewable biomass fuel [38–43]. Municipal waste incineration power is becoming an important new energy generation technology. The temperature of flue gas generated during municipal waste incineration was generally at 150–180 °C. Therefore, developing NH_3-SCR catalyst which could work at ultra-low operation temperature ($\leq$ 200 °C) is highly demanded for municipal waste incineration. In addition, the flue gas of municipal waste incineration includes lots of water vapor ($\geq$25%) and SO_2. Improving the H_2O+SO_2 resistance of NH_3-SCR catalysts was another challenge for deNO_x in municipal waste incineration industry.

The development of NH_3-SCR catalysts has received increasing attention in the past several decades [44,45]. As shown in Fig. 1, the number of publications on the topic of "SCR catalyst" increased dramatically in the past few decades. However, no reviews summarize the challenges of NH_3-SCR catalysts during the energy transition of power generation industry.

In this work, we detailly analyze the development of NH_3-SCR catalysts in electric industries (coal-fired power plants and municipal waste incineration). And subsequently, we further discuss that the general strategies on solving these problems for the different types of catalysts by giving some specific examples. At last, we also

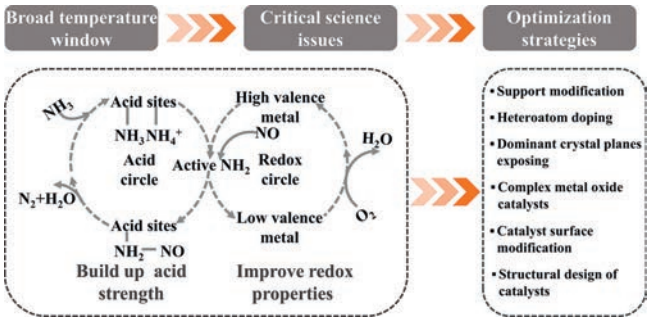

Fig. 2. Reaction mechanism of NH_3-SCR and general strategies for widening operating temperature window of SCR catalysts.

propose the future research challenges and directions of $deNO_x$ in electric industries.

2. SCR catalysts in coal-fired power plants

2.1. Broad temperature window (200–400 °C)

NH_3-SCR technology has become one of the most efficient ways to remove NO_x in coal-fired power plants [46]. However, in order to combat climate change, the electric systems need turn to a low-carbon and sustainable development mode in the near future. The new energy generation plants are gradually replacing traditional power plants. Therefore, the traditional coal-fired power boilers would have to operate under a low load condition. The temperature of flue gas generated in coal-fired power boiler would decrease to about 250 °C under a low-load condition. However, traditional V_2O_5-TiO_2 only could maintain a high catalytic activity in a narrow temperature window (300–400 °C). And it could not meet the demand of future coal-fired power plants. The development of new catalysts and modification of traditional V_2O_5-based catalysts which can work in a broad temperature window has been a pressing demand in coal-fired power industry.

As shown in Fig. 2, in general, the mechanism of standard NH_3-SCR reaction includes acid and redox circle. In terms of L-H mechanism, the NH_3 is absorbed on acid sites to generate NH_4^+, and the active nitrates generated by the oxidation of NO further react with NH_4^+, leading to the generation of NH_4NO_2/NH_4NO_3 species which degrade to N_2 and H_2O. In terms of E-R mechanism, the NH_3 is firstly absorbed on acid sites and dehydrogenated to -NH_2 while the high valence metal is reduced. Subsequently, the -NH_2 reacts with NO to form -NH_2NO which decomposes to N_2 and H_2O to complete the acid circle. The low valence metal is oxidized to high valence by O_2 and further to generate H_2O to complete the redox circle. As is reported [47], the acid and redox circle would significantly slow down with the decrease of reaction temperature. Therefore, how to build up the acid strength of active metal sites and improve their redox properties are the key to improve the catalyst activity of NH_3-SCR catalysts.

The development of catalysts generally focused on traditional V-based oxides, novel Ce/Fe-based oxides and ion-exchanged zeolites. And the general strategies were the surface modification, structural designment of catalyst and so on. According to our statistic in Table 2, most catalysts have achieved high NO_x removal efficiency in a broad-temperature window from 200 °C to 450 °C [48–69].

2.1.1. The modification of V-based catalysts

The traditional V_2O_5/TiO_2 catalyst work within a narrow temperature range between 300 °C and 400 °C, nevertheless, its operating temperature could be broadened by modifying catalyst surface or using catalyst support. Zhao *et al.* [50] reported a S-N doped V_2O_5/TiO_2 catalyst and its NO_x removal efficiency achieved nearly 100% within a temperature range of 240–450 °C. The NH_3-TPD and H_2-TPR curves indicated that the introduction of S-N built up the acid strength of V_2O_5/TiO_2 and enhanced the redox property of V_2O_5/TiO_2 catalyst. In their another publication, Ti^{3+} were introduced to V_2O_5/TiO_2 catalyst to improve its low-temperature catalysis performance [70]. Furthermore, Cao *et al.* [71] found that the co-doping of Ce^{4+} and Zr^{4+} could improve the denitration performance of V_2O_5-WO_3/TiO_2.

The broad temperature performance of V_2O_5-based catalysts could also be improved by modification of catalyst support. The modification of catalyst support can be classified into two groups: the modification of traditional TiO_2 support and the introduction of novel catalyst support.

Lian *et al.* [25] pretreated TiO_2 support at 850 °C and deposited vanadium species on its surface. They found that the NH_3-SCR performance of catalyst using pretreated TiO_2 as the support could achieve nearly 100% $deNO_x$ efficiency at 240 °C and above. Si *et al.* [72] successfully increased the $deNO_x$ efficiency of V_2O_5/TiO_2 under the working temperature of 250–350 °C by doping Sn into rutile TiO_2. Song *et al.* [73] successfully synthesized microporous TiO_2 as the support of V_2O_5 catalyst which enhanced the NO_x conversion to nearly 90% at the working temperature of 250 °C below.

For the design of novel catalyst support, Liu *et al.* [48] prepared ZrO_2 supports with diverse morphologies as the supports of V_2O_5 by self-assembly methods. And they found that the interaction between mesoporous ZrO_2 support and surficial vanadium species is beneficial for the increased proportion of low valence vanadium and absorbed oxygen. And the catalyst activity test indicated that the NO conversion over V/MZ (V_2O_5 deposited on mesoporous ZrO_2) achieved nearly 95% between 225 °C and 425 °C.

2.1.2. The development of Fe-based catalysts

The Fe-based metal oxides as a promising alternative of V-based catalysts have become one of the most efficient catalysts in SCR catalysis due to the Fe^{2+}/Fe^{3+} redox circle [74,75]. The development of Fe-based catalysts generally focused on the control of the morphology and structure as well as the modification of the catalyst surface. The overoxidation of NH_3 under high temperature is another concern for Fe-based catalysts. Wang *et al.* [49] successfully synthesized WO_3-FeO_x catalysts by a solvent-free method. The introduction of WO_3 restrained the growing of the Fe_2O_3 particles and inhibited the agglomeration of the particles. And the NO_x conversion over the catalyst could achieve 90% between 200 °C and 500 °C. Liu *et al.* [76] also found that the addition of WO_x could improve the activity of Fe_2O_3 catalyst by supplying abundant surface reactive Lewis and Bronsted acid sites. The NO_x conversion could achieve 80% above from 300 °C to 450 °C.

Han *et al.* [77] anchored Fe_2O_3–CeO_2 onto the mesoporous Al_2O_3 nanoarrays which were *in situ* created on the surface of Al-mesh. The Al_2O_3 nanoarrays supplied abundant sites for the anchoring of metal oxides catalysts. Furthermore, they also founded that the presence of Ce changed the charge distribution of Fe and the interaction between Ce and Fe benefited NH_3-SCR. Chen *et al.* [65] Introduce the single-atom Ce species to the surface of α-Fe_2O_3 to improve the content of Fe^{2+} and decrease the oxygen vacancy formation energy. NO conversation over the Ce-modified α-Fe_2O_3 was above 95% at a very low temperature of 175 °C.

2.1.3. Metal ion-exchanged zeolite catalysts

The ion-exchanged zeolites are another high-efficiency substitute of traditional V_2O_5/TiO_2 catalysts. In recent years, Cu-based exchanged zeolites have been the most widely studied zeolite catalyst in NO_x removal because its active temperature window could cover low, medium and high temperature [18,20,78–83].

Table 2
The summary about the literature data for widen operating temperature windows on NH_3−SCR reaction.

Type	Catalysts	Reaction condition	The temperature range of T_{90} (°C)	Refs.
V-based	V_2O_5/ZrO_2	0.1% NO, 0.15% NH_3, 2% O_2, GHSV = 30,000 h^{-1}, Ar as balance	200–450	[48]
	$V_2O_5/MoO_3/TiO_2$	0.06% NO, 0.06% NH_3, 3% O_2, WHSV = 72,000 mL $g_{cat.}^{-1}$ h^{-1}, N_2 as balance	200–350	[59]
	S/N-V_2O_5/TiO_2	0.05% NO, 0.05% NH_3, 5% O_2, GHSV = 27,549 h^{-1}, N_2 as balance	218–393	[50]
	3DOM-$Fe_{10-x}V_x$	0.05% NO, 0.05% NH_3, 5% O_2, WHSV = 60,000 mL $g_{cat.}^{-1}$ h^{-1}, N_2 as balance	170–380	[56]
	$MnCoVO_x$	0.05% NO, 0.05% NH_3, 5% O_2, WHSV = 60,000 mL $g_{cat.}^{-1}$ h^{-1}, N_2 as balance	180–470	[64]
Fe-based	$Cu_{0.02}Fe_{0.2}W_aTiO_x$	0.1% NO, 0.1% NH_3, 3% O_2, GHSV =100,000 h^{-1}, N_2 as balance	225–500	[54]
	WO_3-FeO_x	0.06% NO, 0.06% NH_3, 5% O_2, GHSV = 60,000 h^{-1}, N_2 as balance	225–500	[49]
	WO_3/Fe_2O_3	0.06% NO, 0.06% NH_3, 3% O_2, WHSV = 72,000 cm^3 h^{-1} g^{-1}, N_2 as balance	300–500	[52]
	$Fe_{0.93}Ce_{0.07}O_x$	0.05% NO, 0.05% NH_3, 5% O_2, GHSV = 90,000 h^{-1}, N_2 as balance	180–580	[65]
Zeolite	FeCu-SSZ-13	0.05% NO, 0.05% NH_3, 5% O_2, GHSV = 180,000 h^{-1}, N_2 as balance	200–400	[57]
	Cu/Co/Ni-Y zeolite	0.072% NO, 0.08% NH_3, 3% O_2, GHSV = 30,000 h^{-1}, N_2 as balance	175–375	[62]
	Fe/Cu-SSZ-13	0.05% NO, 0.05% NH_3, 5% O_2, GHSV = 30,000 h^{-1}, Ar as balance	160–590	[68]
	Cu-SSZ-13	0.05% NO, 0.05% NH_3, 5% O_2, GHSV = 400,000 h^{-1}, N_2 as balance	200–450	[55]
	Fe-ZSM-5	0.035% NO, 0.0385% NH_3, 15% O_2, GHSV = 60,000 h^{-1}, N_2 as balance	150–550	[58]
	Cu-SAPO-44	0.05% NO, 0.05% NH_3, 5.3% O_2, GHSV = 100,000 h^{-1}, He as balance	300–550	[61]
	Cu-(Mn)-UZM-9	0.05% NO, 0.05% NH_3, 5% O_2, GHSV = 100,000 h^{-1}, N_2 as balance	200–650	[69]
Ce-based	CeO_2-TiO_2-ZrO_2	0.072% NO, 0.08% NH_3, 3% O_2, GHSV = 30,000 h^{-1}, N_2 as balance	218–393	[51]
	MnCe/Ti-VW/Ti	0.05% NO, 0.05% NH_3, 5% O_2, GHSV = 36,000 h^{-1}, N_2 as balance	190–410	[53]
	P-Ce-Zr-Ti	0.072% NO, 0.08% NH_3, 3% O_2, GHSV = 30,000 h^{-1}, N_2 as balance	200–375	[60]
	TiO_2@$CeMnO_x$	0.05% NO, 0.05% NH_3, 5% O_2, GHSV = 30,000 h^{-1}, N_2 as balance	200–400	[63]
	$MoO_3/CeZrO_x$	0.05% NO, 0.055% NH_3, 5% O_2, GHSV = 30,000 h^{-1}, N_2 as balance	225–460	[67]
	CoCeTi	0.05% NO, 0.05% NH_3, 5% O_2, GHSV = 100,000 h^{-1}, N_2 as balance	250–450	[66]

Sun *et al.* [84] investigated the influence of Si/Al ratio on NH_3-SCR activity of Cu-SSZ-13 zeolite, and found that the Si/Al ratio or Cu loadings could influence the hydrothermal stability and catalytic activity of Cu-SSZ-13 zeolite by controlling the formation of Cu^{2+}–2Al and $[Cu^{II}(OH)]^+$–Al. Jin *et al.* [62] reported that the existence of Cu species on zeolite surface could promote the adsorption and activation of NH_3. And their NH_3-SCR activity test result indicated that the T_{90} (temperature window of NO_x conversion $\geq$ 90%) temperature window was 200–350 °C. Daya *et al.* [85] developed the kinetic model of the Cu^I/Cu^{II} redox circle during NH_3-SCR. Wang *et al.* [86] prepared Cu-ZSM-5 catalysts with different morphologies (nanosheets, nanoparticles and hollow spheres). They found that the NO conversion over nanosheet-like Cu-ZSM-5 (NS-Cu-CZSM-5) could achieved nearly 100% in the temperature window from 200 °C to 400 °C. Furthermore, they also found that Cu-based zeolite contains CuO and CuO is bad for NO reduction. Several strategies have been reported in inhibiting the growth of CuO crystal. Zhang *et al.* [87] suppressed the generation of CuO by increasing the amounts of acidic sites in zeolite structure. They widened the T_{90} of Cu exchanged zeolite to 200–600 °C. Ma *et al.* [88] reported that the formation of CuO in Cu-SSZ could be restrained by surface Al modification. And the T_{90} temperature range could be widened to 200–500 °C. Yue *et al.* [57] successfully restrained the generation and growth of CuO grains by Fe modification. And the NO conversion over FeCu-SSZ-13 could achieved above 95% within the temperature range of 200–550 °C. Except for Cu, some metal ions such as Fe and Ce also are attractive compensation ion for zeolite catalysts. Shi *et al.* [89] reported the NO_x conversion over In and Ce bimetallic catalyst supported by zeolite nearly achieved 100% within the temperature range of 250–600 °C. Liu *et al.* [90] reported a Fe-Ni-W zeolite catalyst and investigated its NH_3-SCR activity in a wide temperature window of 200 °C–850 °C.

In recent years, some researchers are trying to synthesize and develop zeolites with different framework structure as NH_3-SCR catalysts. Tarach *et al.* [80] studied the influence of zeolite topology on NH_3-SCR activity and found that topology structure could affect the redox circle between Cu^{2+} and Cu^0. Zhang *et al.* [91] reported a new CHA-type aluminoborosilicates and applied it to deNO_x reaction. The T_{90} temperature range of the catalyst could be widened to 200–500 °C. Chitac *et al.* [92] synthesized a small-pore SWY zeolite and further introduced Cu to zeolite framework structure. The NH_3-SCR light-off test indicated that the catalyst could achieve 90% NO_x conversion between 200 °C and 500 °C.

In conclusion, in consideration of vanadium biotoxicity, developing novel vanadium-free catalysts working in a wide active temperature window has been a research hotspot. The critical factors which affect the performance of SCR catalysts are acid site strength and redox properties. The general strategies to improve acid site strength and redox property included doping modification, grain growth control and dominant crystal planes exposure. In recent years, some novel NH_3-SCR catalysts such as Fe-, Ce-based catalysts have been widely reported. However, the synthesis methods of these catalysts involve fancy instruments and require accurate parameter control. As a result, how to simplify the preparation procedures of the catalysts is critical for the mass production of novel vanadium-free deNO_x catalysts.

2.2. Improve the SO_2 resistance of SCR catalysts

Many studies have shown that the presence of SO_2 in the flue gas from coal-fired plants negatively influence the catalytic activity of SCR catalysts. The negative effects of SO_2 on SCR catalysts include physical deactivation and chemical deactivation. The physical deactivation was caused by the deposition of NH_4HSO_4 (ABS) over catalysts surface [32] while the chemical deactivation was the sulfation of active sites. In particular, the physical deactivation could be the main problem when the working temperature of deNO_x was below 300 °C. ABS becomes a very viscous liquid (0.1–0.2 Pa·s) within the temperature range of 147–350 °C [93,94] and sticks to the surface of catalysts with coal ash, leading to the reactor channel being blocked. As described in Fig. 3, the generation of ABS proceed *via* three main steps: the adsorption of SO_2, the oxidation of SO_2 and the binding of NH_4^+ and HSO_4^-. The general strategies to improve the SO_2 resistance of catalysts focused on inhibiting the adsorption and oxidation of SO_2 and promoting the decomposition of ABS. In Table 3, We made a summary about the strategies to improve the SO_2 resistance of NH_3-SCR catalysts.

2.2.1. Inhibiting the adsorption of SO_2

Inhibiting the adsorption of SO_2 on the surface of catalysts was an important strategy to directly curb the generation of

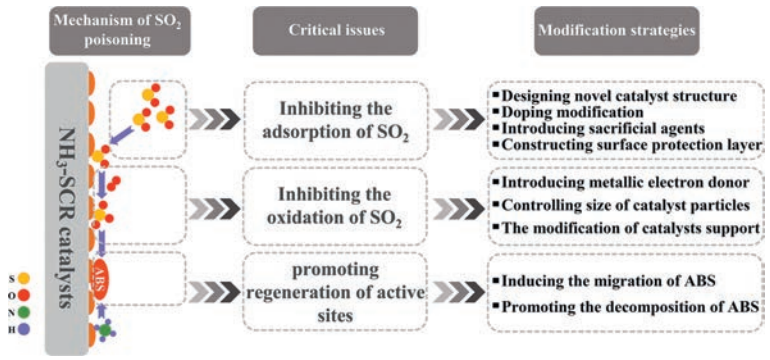

Fig. 3. The poisoning mechanism of SO_2, and general modification strategies of SO_2 resistance.

Table 3
The summary for the published works which improved SO_2 resistance by different strategies.

Strategies	Catalyst	Reaction condition	The performance of SO_2 resistance	Refs.
Inhibiting the adsorption of SO_2	$MnCoO_x$	0.05% NH_3, 0.05% NO, 5% O_2, 0.005% SO_2, 140,000 h^{-1}, 175 °C	90% for 12 h, reversible	[101]
	CeO_2-SiO_2	0.05% NH_3, 0.05% NO, 5% O_2, 0.05% SO_2, 48,000 h^{-1}, 250 °C	≥90% for 40 h, reversible	[100]
	$Fe_\delta Ce_{1-\delta}VO_4$	0.05% NH_3, 0.05% NO, 5% O_2, 0.01% SO_2, 60,000 h^{-1}, 240 °C	≥80% for 22 h	[99]
	S-Fe_2O_3@CeO_2/TiO_2	0.05% NH_3, 0.05% NO, 5% O_2, 0.02% SO_2, 30,000 h^{-1}, 250 °C	≥70% for 13 h	[103]
	Ce-MnO_2	0.05% NH_3, 0.05% NO, 5% O_2, 0.025% SO_2, 30,000 h^{-1}, 150 °C	≥70% for 6 h	[104]
	Fe/Co-Mn-Ce/TiO_2	0.05% NH_3, 0.05% NO, 5% O_2, 0.02% SO_2, 12,000 h^{-1}, 200 °C	≥95% for 9 h	[98]
Inhibiting the oxidation of SO_2	CeO_2/MoO_3	0.05% NH_3, 0.05% NO, 3% O_2, 0.1% SO_2, 280 °C	100% for 20 h	[105]
	$MnCeSmTiO_x$	0.05% NH_3, 0.05% NO, 5% O_2, 0.02% SO_2, 5% H_2O, 80,000 h^{-1}, 260 °C	≥80% for 5 h	[106]
	Cu-CeV-Ce-WTi	0.03% NH_3, 0.03% NO, 5% O_2, 60,000 h^{-1}, 220 °C	≥80% for 20 h	[107]
	Sm-$MnFeO_x$	0.05% NH_3, 0.05% NO, 5% O_2, 0.01% SO_2, 60,000 h^{-1}, 200 °C	≥90% for 7 h	[108]
	Co-CeMn	0.03% NH_3, 0.03% NO, 5% O_2, 0.01% SO_2, 10% H_2O, 60,000 h^{-1}, 210 °C	≥90% for 6 h	[109]
	Ce-α Fe_2O_3	0.05% NH_3, 0.05% NO, 5% O_2, 0.02% SO_2, 5% H_2O, 60,000 h^{-1}, 250 °C	≥90% for 180 h	[65]
Promoting the regeneration of catalytic active sites	VWCeTi	0.08% NH_3, 0.08% NO, 3% O_2, 0.05% SO_2, 6% H_2O, 30,000 h^{-1}, 220 °C	100% for 100 h	[36]
	VWTi+Zeolite	0.06% NH_3, 0.05% NO, 10% O_2, 0.003% SO_2, 10% H_2O, 150,000 h^{-1}, 220 °C	≥70% for 20 h	[118]
	VWTi+Al	0.06% NH_3, 0.05% NO, 10% O_2, 0.01% SO_2, 10% H_2O, 100,000 h^{-1}, 220 °C	≥60% for 20 h	[27]
	Fe_2O_3-MoO_3	0.05% NH_3, 0.05% NO, 3% O_2, 0.0145% SO_2, 10% H_2O, 33,000 h^{-1}, 280 °C	13% for 25 h	[114]
	Fe_2O_3/SBA-150	0.05% NH_3, 0.05% NO, 5% O_2, 0.08% SO_2, 15,000 h^{-1}, 250 °C	≥50% for 18 h	[37]
	MoO_3/TiO_2	0.06% NH_3, 0.06% NO, 3% O_2, 0.02% SO_2, 72,000 h^{-1}, 250 °C	≥60% for 80 h	[116]

ABS [95–98]. The SO_2 adsorption could be inhibited by introducing some special catalytic promoters, constructing sacrificial sites, creating protection layer and so on. The catalytic promoter which could strengthen the acidity or weaken the alkalinity of active sites is beneficial for inhibiting SO_2 adsorption because SO_2 is atypical acidic oxide. Some nonmetal elements or metal elements with strong electronegativity are always good options. Kang *et al.* [99] found that the introduction of Fe into $CeVO_4$ could restrain the adsorption of SO_2 by increasing the types and amounts of acidic sites. The long-term NH_3-SCR test in the presence of 100 ppm SO_2 showed that the NO conversion over $Fe_\delta Ce_{1-\delta}VO_4$ could maintain above 80% after 25 h. Tan *et al.* [100] successfully synthesized innovative CeO_2-SiO_2 mix oxide using coprecipitation method. The strong interaction of Ce-O-Si weaken the alkalinity of CeO_2 and further inhibited the adsorption of SO_2 on Ce. The catalytic stability tests in the presence of 500 ppm SO_2 indicated that the NO conversation over CeO_2–SiO_2 could still maintain about 90% after 40 h aging. Chen [101] introduced Co species into MnO_x and found that the NO_x conversion over Co-modified MnO_x could be kept at above 85% in the presence of 50 ppm SO_2 for 10 h (Fig. 4a). Park *et al.* [102] introduced Nb and Mo to VO_x-oxide and kept NOx conversion above 80% after 124 h in the presence of 500 ppm SO_2.

Moreover, creating protective layer or introducing sacrificial agents could also protect metallic active sites from the harm of SO_2 adsorption. Qi *et al.* [103] deposited a layer of iron sulfate on the surface of CeO_2/TiO_2 catalyst. The presence of surface iron sulfate cut off SO_2 adsorption pathway and inhibited the sulfation of Ce species (Fig. 4b). Fang *et al.* [104] doped Ce atoms into MnO_2 as the sacrificial sites of SO_2 adsorption and oxidation. Furthermore, they found that the generation of $Ce_2(SO_4)_3$ could supply extra adsorption sites for NH^{4+} to upgrade the reaction of NO_x reduction. Tang [97] prepared a protect layer of amorphous MoO_x on the surface of $CeFeO_x$ and the NO_x conversion could maintain above 90% in the presence of SO_2 for 60 h.

2.2.2. Inhibiting the oxidation of SO_2

The SO_2 resistance of catalysts could also be improved by inhibiting the oxidation of SO_2 [105–109]. The key to restrain SO_2 oxidation is suppressing the electron transfer from SO_2 to metal active centers. Some researchers are trying to confining active metal species on nanoscale catalyst support to achieve this goal. Hu *et al.* [105] successfully prepared highly dispersed ceria particles by loading CeO_2 onto the surface of MoO_3 nanorod support. And the percentage of Ce^{3+} increased from 9% (bulk CeO_2) to 60% (CeO_2/MoO_3) (Fig. 4c). The catalyst could maintain nearly 100% NO conversion in the presence of 1000 ppm SO_2 for 20 h at 280 °C. Xu *et al.* [110] confined active Cu species in TiO_2 nanotubes and successfully improve the Cu^+/Cu^{2+} ratio. The NO_x conversion of the catalyst could keep above 80% after 100 ppm SO_2 poisoning test of 8 h. Wang *et al.* [111] synthesized Ce-based catalyst which used montmorillonite/TiO_2 composite as the support. The NO conversion over the catalyst still maintained above 80% in the presence of 100 ppm SO_2 after 5 h test.

Furthermore, constructing facile electron transfer pathway by introducing electron donor could also suppress the electron transfer between SO_2 and active metal sites. Wang *et al.* [106] doped Sm into $MnCeTiO_x$ catalyst to inhibit SO_2 oxidation by Mn^{4+} and Ce^{4+}. The electron transfer pathways of $Sm^{2+} \rightarrow Mn^{4+}$ and $Sm^{2+} \rightarrow Ce^{4+}$

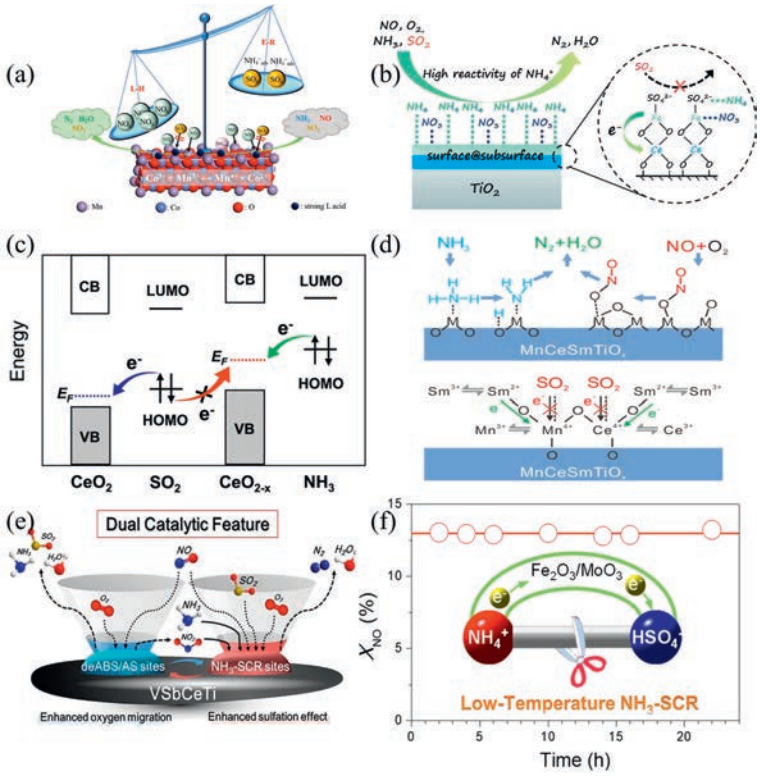

Fig. 4. Schematic illustration of (a, b) inhibiting adsorption of SO_2. Reprinted with permission [101]. Copyright 2023, Elsevier. Reprinted with permission [103]. Copyright 2022, American Chemical Society. (c, d) inhibiting oxidation of SO_2. Reprinted with permission [105]. Copyright 2021, American Chemical Society. Reprinted with permission [106]. Copyright 2020, American Chemical Society. (e, f) promoting regeneration of active sites. Reprinted with permission [36]. Copyright 2021, Elsevier. Reprinted with permission [114]. Copyright 2018, American Chemical Society.

suppressed the electron transfer between SO_2 and Mn^{4+}/Ce^{4+} (Fig. 4d). Purbia *et al.* [107] doped CuO–CeO_2 nano-heterostructures to V_2O_5–CeO_2–WO_3/TiO_2 catalysts to improve SO_2 resistance of V_2O_5-based catalysts. They found that the facile electron transfer between Cu-Ce and V restrained the oxidation of SO_2 on the surface of active sites. Xu *et al.* [112] prepared a MnCe/GAC–CNTs catalyst with excellent SO_2 resistance. And the electron transfer between Ce and Mn restrained the oxidation of SO_2.

2.2.3. Promoting the regeneration of catalytic active sites

Because the decomposition temperature of ABS was above 350 °C, the deposition of ABS on catalyst surface was unavoidable while the system was running below 300 °C. Removing ABS from catalyst surface was critical for the regeneration of active sites covered by ABS. The general strategies are promoting the decomposition of ABS or inducing the migration of ABS [37,113–115].

Kwon *et al.* [36] found that the decomposition of ABS/AS was related with the oxygen vacancies and reactive oxygen species in catalysts (Fig. 4e). They added Sb-Ce to V_2O_5/TiO_2 and found that the introduction of Sb-Ce could improve the ratio of unstable O_α species. And further the decomposition temperature of ABS would decrease from 300 °C above to 264 °C. Chen [114] successfully synthesized Fe_2O_3 on the surface of α-MoO_3 nanobelts (Fig. 4f). The α-MoO_3 with the structure of nanobelt could trap NH_4^+ from ABS and promote the decomposition of ABS. Guo *et al.* [116] found that MoO_3 could capture NH_4^+ to promote the decomposition of ABS. Guo *et al.* successfully prepared sub-monolayer MoO_3 on the surface of TiO_2 and found that the atomically dispersed O-Mo-O could effectively improve the decomposition of ABS on TiO_2. Chen *et al.* [117] prepared a TiO_2-support single-atom Mo catalyst and successfully decreased the decomposition temperature of ABS to 225 °C.

Inducing the migrant of ABS is another effective strategy to remove the ABS on catalyst surface. Song *et al.* [118] physically mixed H-Y zeolite with V_2O_5/TiO_2 and used H-Y zeolite as a trapper of ABS to protect vanadium active sites. The regeneration and reusability test indicated that the VWTi+Z catalyst aged for 20 h by SO_2 could achieve almost the same performance with fresh catalyst after regeneration at 350 °C. Jeon *et al.* [27] used alumina as the trapper of ABS to protect V_2O_5/WO_3-TiO_2 catalyst. And the catalyst could almost totally regeneration after calcining at 350 °C.

Inhibiting AS/ABS deposition is critical to improve SO_2 resistance of catalysts at low temperature below 300 °C. The general strategies adopted in previous studies were cutting off the generation pathway of AS/ABS and removing AS/ABS from catalyst surface. However, flue gas is a complex mixture which include water vapor, CO_2, particulates, alkali/alkaline/heavy metals, SO_2 and NO_x. And there are still lack of related studies about the poisoning mechanism of muti-pollutants coexistence. It is important for the developing of NH_3-SCR which have excellent poisoning resistance.

3. Recent progress of SCR catalyst in municipal waste incineration

3.1. Ultra-low temperature SCR catalysts (≤200 °C)

As a promising substitute of traditional power generation, biomass combustion power generation has gained increasing attention. The municipal waste incineration as a source of renewable biomass energy is gradually becoming an important power generation technology. However, the deNO_x treatment of flue gas in municipal waste incineration power plants restrained its development. The temperature of flue gas from municipal waste incineration power plants generally ranges between 100 °C and 200 °C, and can

Table 4
The summary about the performance of catalysts under ultra-low temperature condition.

Type	Catalysts	Prepared method	Reaction condition	The temperature range of T_{90} (°C)	Refs.
Mn-based	OMS-5(H)@TiO_2	Hydrothermal method	0.05% NO, 0.05% NH_3, 5% O_2, 40,000 h^{-1}	90–240	[119]
	$V_\alpha-MnO_x$	Sol-gel method	0.05% NO, 0.05% NH_3, 5.3% O_2, 50,000 h^{-1}	120–240	[120]
	Co-MnO_x	Solvothermal approach	0.2% NO, 0.2% NH_3, 8% O_2, 32,000 h^{-1}	75–200	[123]
	Sn-MnO_x-CeO_2	Ultrasonication-assisted coprecipitation method	0.1% NO, 0.1% NH_3, 2% O_2, 35,000 h^{-1}	70–250	[124]
	β-MnO_2	Calcinating γ-MnO_2 precursor	0.05% NO, 0.05% NH_3, 5% O_2, 160,000 h^{-1}	100–350	[125]
	MnO_x-Ac^-	*In situ* deposition	0.1% NO, 0.1% NH_3, 3% O_2, 105,000 h^{-1}	100–300	[126]
	$SmMnO_5$	Hydrothermal method	0.05% NO, 0.05% NH_3, 5% O_2, 50,000 h^{-1}	90–210	[78]
	$TiSmMnO_x$	Coprecipitation	0.05% NO, 0.05% NH_3, 5% O_2, 50,000 h^{-1}	75–225	[114]
	$MnCeWO_x$	Homogeneous precipitation method	0.05% NO, 0.05% NH_3, 5% O_2, 100,000 h^{-1}	125–250	[127]
	Ce-$MnCrO_x$-LDO	Coprecipitation	0.05% NO, 0.05% NH_3, 5% O_2, 90,000 h^{-1}	150–250	[128]
	$Fe_{0.35}Mn_{2.65}O_4$	Confinement–pyrolysis–oxidation strategy	0.06% NO, 0.06% NH_3, 5% O_2, 200,000 h^{-1}	140–290	[129]
Ce-based	Nb_2O_5/CuO/CeO_2	Incipient wetness impregnation (IWI)	0.05% NO, 0.05% NH_3, 10% O_2, 250,000 h^{-1}	150–350	[130]

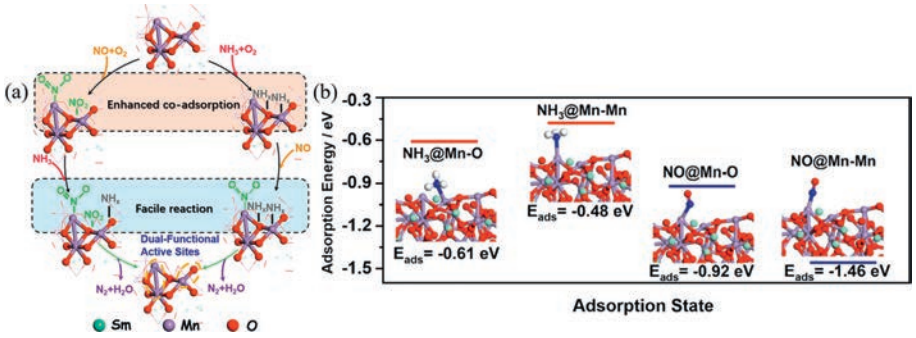

Fig. 5. Schematic illustration of (a, b) the NH_3-SCR reaction over the SM-E catalyst. Reprinted with permission [131]. Copyright 2022, American Chemical Society.

not reach the ignition temperature of traditional V_2O_5-based catalysts. Compared with other types of deNO_x catalysts, MnO_x-based catalysts could exhibit excellent deNO_x efficiency under ultra-low temperature condition (≤200 °C) [119–122]. Table 4 summarizes the NH_3-SCR catalysts working under ultra-low temperature condition. The modifications of MnO_x catalysts include structure or morphology modification of single MnO_x, construction of MnO_x-based composite oxides and the construction of core-shell structure [78,114,119,120,123–130].

The crystallinity is one of the most important factors which affect the activity of catalysts. The low crystallinity benefited the generation of oxygen defects on catalysts. Therefore, most studies focused on decreasing the crystallinity of MnO_2 to improve the catalytic activity of MnO_2. Yang *et al.* [125] successfully reduced the crystallinity of MnO_2 by a facile procedure of phase transformation. According to the HRTEM and XPS results of β-MnO_2, the considerable amounts of defects and the high concentrations of surface absorbed oxygen were detected, indicating that the concentrations of oxygen defects were increased in β-MnO_2 compared with that in γ-MnO_2. Furthermore, NO conversation over β-MnO_2 could maintain almost 100% NO conversation when the working temperature was decreased to 150 °C. Zhang [126] successfully synthesized an amorphous MnO_x by *in-situ* deposition as the catalyst of deNO_x reaction, which exhibited excellent performance for low temperature deNO_x.

However, the working temperature windows of single MnO_x catalysts are very narrow. Lots of efforts have been devoted to broaden the working temperature windows of MnO_x catalysts. Construction of MnO_x-based composite oxides was an effective method to widen the working temperature of MnO_x. Some transition or lanthanide metals (Ce, Fe, Sm, Gd, *etc.*) have been introduced to combine with MnO_x. Wang [131] introduced Sm to MnO_x and subsequently erased Sm atoms from $SmMnO_x$ by nitric acid.

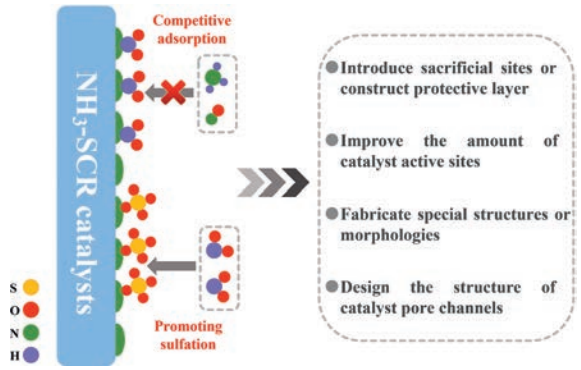

Fig. 6. The poison mechanism of H_2O and general strategies for improving H_2O resistance.

They found that the removal of Sm led to the exposure of Mn-O and Mn-Mn dual-functional sites and the increased Mn^{4+}/Mn^{3+} ratio (Figs. 5a and b). They also found that the NO conversation over $SmMnO_5$ after being treated by nitric acid could maintain about 100% in a very wide temperature window from 80 °C to 210 °C. Xu *et al.* [132] found doping Ti and Sm to MnO_x widened the optimal working temperature from 170–210 °C to 70–230 °C. Geng *et al.* [127] successfully prepared W-Mn_3CeO_x which showed a good SCR activity at the temperature of 120–260 °C.

In conclusion, Mn-based catalyst has become one of the most potential catalysts which could directly catalyze NH_3-SCR process under ultra-low temperature condition. The studies about widening active temperature window and improving N_2 selectivity of MnO_x-based catalysts have made a great progress in recent years. However, a lot of components including alkali/alkaline-earth/heavy

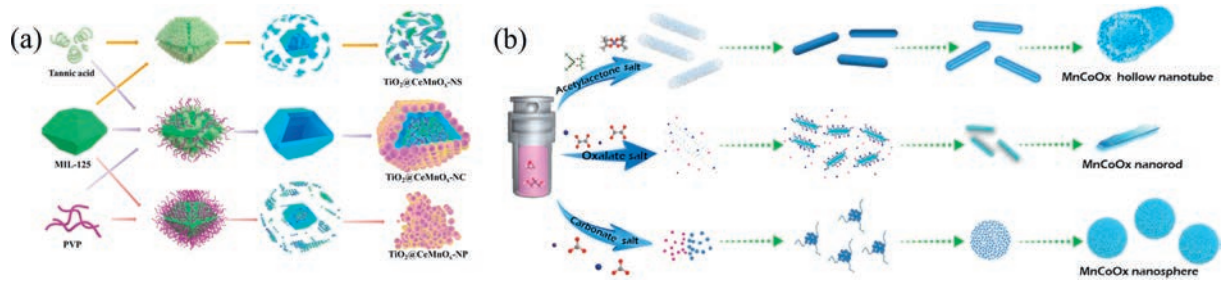

Fig. 7. (a) Illustration of the hydrolysis etching and construction for $CeMnTiO_x$. Reprinted with permission [63]. Copyright 2022, Elsevier. (b) Schematic illustration of the formation of $MnCoO_x$ oxides. Reprinted with permission [134]. Copyright 2021, Elsevier.

metals (Mg, K, Na, Hg, *etc.*) and acidic compounds (HCl, HF, *etc.*), abundantly existed in the flue gas could cause the deactivation of Mn-based catalyst. Improving the poison resistance of Mn-based catalyst can be the focus of future studies.

3.2. SO_2+H_2O resistance

The $deNO_x$ catalysts composed by MnO_x-based oxides always show terrible stability in the presence of H_2O and SO_2. However, the combustion of municipal waste incineration produces a large number of water vapor (≥25%) and SO_2. MnO_x-based oxides has become one of the most promising $deNO_x$ catalysts in municipal waste incineration industry. How to improve the stability of MnO_x-based catalysts in the presence of H_2O+SO_2 was another urgent issue which need be tackled for the development of $deNO_x$ catalysts in municipal waste incineration industry [2,104,133–135]

Fig. 6 shows the deactivation mechanism of $deNO_x$ catalysts in the presence of H_2O+SO_2. Water vapor can compete for active sites with reactants and aggravate the poisoning effect of SO_2.

The general strategies to improve H_2O+SO_2 resistance of MnO_x catalysts are also described in Fig. 6. Introducing sacrificial or protective layer was one of the most effective strategies to inhibit the influence of H_2O+SO_2. Huang *et al.* [63] constructed a TiO_2 nanocage on the surface of $CeMnO_x$ by directional hydrolytic etching of MIL-125 (Fig. 7a). The as-prepared $CeMnO_x$ exhibited excellent water vapor resistance under the protection of TiO_2 nanocages. Song *et al.* [136] also achieved protective effect by introducing Ce-Ti as the sacrificial sites of H_2O and SO_2 adsorption. Furthermore, improving the amounts of active sites was another effective strategy [134]. Raja *et al.* [137] modified Mn/TiO_2 catalyst by the introducing of CNTs and Cu. Their results demonstrated that the incorporation of CNTs and Cu increased the amount and acidity of active sites on the MnO_x. In addition, fabricating special structures or optimizing the pore channel of catalysts could also improve the H_2O+SO_2 resistance of deNOx catalysts. Shi *et al.* [134] successfully synthesized a $MnCoO_x$ catalyst with the unique hollow nanotube structure (Fig. 7b). They found that the unique structure of catalyst well protected the active sites in the inner surface from the poisoning of H_2O+SO_2. The NO_x conversion over $MnCoO_x$ could maintain above 80% for a long time in the presence of 10% H_2O and 100 ppm SO_2.

All in all, the general strategies for improving H_2O+SO_2 resistance of Mn-based catalyst focused on inhibiting the adsorption of vaporous H_2O for now. However, the liquefaction of water vapor would happen with the decrease of working temperature. And the liquid film of H_2O would cover the surface of catalyst and cut off reaction pathway. Therefore, in order to apply the Mn-based catalyst in the industrial practices in the future, the new problems caused by the state change of H_2O will be a concern.

4. Conclusion and perspective

In conclusion, this review discussed the challenges SCR catalysts are facing in Coal-fired power plants which operate under low-load conditions and SCR catalysts are facing in municipal waste incineration. The studies on broadening working temperature range and improving the SO_2 resistance of SCR catalysts are summarized in coal-fired power plants which operate under low-load conditions and in municipal waste incineration comprehensively.

Although the studies on SCR catalysts have made a great progress, there are still some research directions which should be focused on:

(1) It is generally accepted that the reaction pathway of NH_3-SCR is controlled by L-H and E-R mechanism. However, which mechanism plays a leading role at specific working temperature have not been identified. In the future, the reaction mechanisms of NH_3-SCR should be studied at different working temperature. The related mechanism studies are the guidance of developing novel SCR catalysts which are adapted to specific working temperature.
(2) For now, the industrial application of powder NH_3-SCR catalysts is generally achieved by assembling monolithic catalysts. The main strategy is to coat catalysts on the surface of base materials. However, there are some problems which restrain the further development of monolithic catalysts in industry. The low utilization rate of catalyst coating results in limited $deNO_x$ efficiency. Furthermore, the catalyst coating is easily to drop off due to low interface strength between powder catalysts and supports. These problems have been ignored during the development of catalysts for a long time. The following research directions are deserved to be focused on: how to choose suitable base materials and control the interface between base and catalyst coating; how to design and optimize the structure and reaction channel; the mass and heat transfer studies of the whole reactors; the construction of simulation models for screening and optimizing monolithic structure.
(3) Considering the complex components of industry flue gas, how to improve the catalytic performance of catalysts in terms of multi-pollutants degradation is a prospective research direction. Developing novel catalysts which could efficiently eliminate the multi-pollutants simultaneously is the optimal strategy to simplify the devices and decrease the costs.

Declaration of competing interest

The authors declare that they have no known competing financial interests or personal relationships that could have appeared to influence the work reported in this paper.

Acknowledgments

This work was financially supported by the National Natural Science Foundation of China (No. 52072306) and the National Key R&D Program of China (No. 2021YFB3701500), and the Fundamental Research Funds for the Central Universities (Nos. 3102019PJ008 and 3102018JCC002).

References

[1] Y. Liu, L. Liu, Y. Wang, Environ. Sci. Technol. 55 (2021) 9691–9710.
[2] G. Xu, X. Guo, X. Cheng, et al., Nanoscale 13 (2021) 7052–7080.
[3] L. Zhang, Y. Wang, C. Feng, et al., Sci. Total Environ. 770 (2021) 145242.
[4] Y. Huang, M. Zhu, M. Ji, et al., Am. J. Respir. Crit. Care Med. 204 (2021) 817–825.
[5] A. Bettiol, E. Gelain, E. Milanesio, et al., Environ. Health 20 (2021) 46.
[6] Z. Khorrami, M. Pourkhosravani, M. Rezapour, et al., Sci. Rep. 11 (2021) 9239.
[7] X. Lu, T. Yao, Y. Li, et al., Environ. Pollut. 212 (2016) 135–146.
[8] Z. Zong, C. Tian, J. Li, et al., Environ. Sci. Technol. 54 (2020) 7787–7797.
[9] Z. Zong, X. Wang, C. Tian, et al., Environ. Sci. Technol. 51 (2017) 5923–5931.
[10] X. Bo, M. Jia, X. Xue, et al., Nat. Sustain. 4 (2021) 811–820.
[11] L. Li, C. Tang, X. Cui, et al., Angew. Chem. Int. Ed. 60 (2021) 14131–14137.
[12] H. Liu, J. Park, Y. Chen, et al., ACS Catal. 11 (2021) 8431–8442.
[13] K. Masera, A.K. Hossain, Fuel 298 (2021) 120826.
[14] D. Wang, Q. Chen, X. Zhang, et al., Environ. Sci. Technol. 55 (2021) 2743–2766.
[15] G. Song, Y. Xiao, Z. Yang, et al., Fuel 292 (2021) 120276.
[16] A. Talaiekhozani, S. Rezania, K.H. Kim, et al., J. Clean. Prod. 278 (2021) 123895.
[17] Y.W. Wu, X.Y. Zhou, J.L. Zhou, et al., Sci. Total Environ. 857 (2023) 159712.
[18] T. Andana, K.G. Rappé, F. Gao, et al., Appl. Catal. B 291 (2021) 120054.
[19] B. Ye, B. Jeong, M.J. Lee, et al., Nano Converg. 9 (2022) 51.
[20] Y. Shan, J. Du, Y. Zhang, et al., Natl. Sci. Rev. 8 (2021) nwab010.
[21] W. Shan, H. Song, Catal. Sci. Technol. 5 (2015) 4280–4288.
[22] W. Shan, Y. Yu, Y. Zhang, et al., Catal. Today 376 (2021) 292–301.
[23] G. Busca, L. Lietti, G. Ramis, et al., Appl. Catal. B 18 (1998) 1.
[24] I. Malpartida, O. Marie, P. Bazin, et al., Appl. Catal. B 113-114 (2012) 52–60.
[25] Z. Lian, J. Wei, W. Shan, et al., J. Am. Chem. Soc. 143 (2021) 10454–10461.
[26] G. Xu, H. Li, Y. Yu, et al., Environ. Sci. Technol. 56 (2022) 3710–3718.
[27] S.W. Jeon, I. Song, H. Lee, et al., Chem. Eng. J. 433 (2022) 133836.
[28] Z. Lian, L. Liu, C. Lin, et al., Environ. Sci. Technol. 56 (2022) 9744–9750.
[29] J. Cao, C. Nannuzzi, W. Liu, et al., Fuel 328 (2022) 125262.
[30] S. Xiong, J. Chen, H. Liu, et al., Environ. Sci. Technol. 56 (2022) 3739–3747.
[31] G. Msigwa, J.O. Ighalo, P.S. Yap, Sci. Total Environ. 849 (2022) 157755.
[32] K. Guo, J. Ji, W. Song, et al., Appl. Catal. B 297 (2021) 120388.
[33] K. Guo, J. Ji, R. Osuga, et al., Appl. Catal. B 287 (2021) 119982.
[34] Y. Yu, W. Tan, D. An, et al., Appl. Catal. B 281 (2021) 119544.
[35] Z. Zhang, R. Li, M. Wang, et al., Appl. Catal. B 282 (2021) 119542.
[36] D.W. Kwon, D.H. Kim, S. Lee, et al., Appl. Catal. B 289 (2021) 120032.
[37] K. Guo, G. Fan, D. Gu, et al., ACS Appl. Mater. Interfaces 11 (2019) 4900–4907.
[38] A.V. Shah, V.K. Srivastava, S.S. Mohanty, et al., J. Environ. Chem. Eng. 9 (2021) 105717.
[39] A.T. Hoang, P.S. Varbanov, S. Nižetić, et al., J. Clean. Prod. 359 (2022) 131897.
[40] N. Kundariya, S.S. Mohanty, S. Varjani, et al., Bioresour. Technol. 342 (2021) 125982.
[41] S. Nanda, F. Berruti, J. Hazard. Mater. 403 (2021) 123970.
[42] S. Khan, R. Anjum, S.T. Raza, et al., Chemosphere 288 (2022) 132403.
[43] T. Rasheed, M.T. Anwar, N. Ahmad, et al., J. Environ. Manag. 287 (2021) 112257.
[44] T. Andana, K. Rappé, F. Gao, et al., Appl. Catal. B 291 (2021) 120054.
[45] J. Wang, H. Zhao, G. Haller, et al., Appl. Catal. B 202 (2017) 346–354.
[46] S. Zhao, J. Peng, R. Ge, et al., Fuel Process. Technol. 236 (2022) 107432.
[47] L. Han, S. Cai, M. Gao, et al., Chem. Rev. 119 (2019) 10916–10976.
[48] S. Liu, H. Wang, Y. Wei, et al., ACS Appl. Mater. Interfaces 11 (2019) 22240–22254.
[49] H. Wang, P. Ning, Y. Zhang, et al., J. Hazard. Mater. 388 (2020) 121812.
[50] W. Zhao, S. Dou, K. Zhang, et al., Chem. Eng. J. 364 (2019) 401–409.
[51] P. Gong, J. Xie, D. Fang, et al., Chem. Eng. J. 356 (2019) 598–608.
[52] J. Zhang, Z. Huang, Y. Du, et al., Chem. Eng. J. 381 (2020) 122668.
[53] Y. Pan, B. Shen, L. Liu, et al., Fuel 282 (2020) 118834.
[54] S. Ma, X. Zhao, Y. Li, et al., Appl. Catal. B 248 (2019) 226–238.
[55] Y. Shan, J. Du, Y. Yu, et al., Appl. Catal. B 266 (2020) 118655.
[56] Y. Li, W. Liu, R. Yan, et al., Appl. Catal. B 268 (2020) 118455.
[57] Y. Yue, B. Liu, P. Qin, et al., Chem. Eng. J. 398 (2020) 125515.
[58] J. Shi, Y. Zhang, Y. Zhu, et al., J. Catal. 378 (2019) 17–27.
[59] Z. Huang, S. Guo, W. Chen, et al., Chem. Eng. J. 464 (2023) 142540.
[60] P. Gong, J. Xie, D. Fang, et al., Appl. Surf. Sci. 505 (2020) 144641.
[61] Y. Xin, N. Zhang, X. Wang, et al., Catal. Today 332 (2019) 35–41.
[62] Q. Jin, D. Fang, Y. Ye, et al., Appl. Surf. Sci. 600 (2022) 154075.
[63] X. Huang, F. Dong, G. Zhang, et al., Chem. Eng. J. 432 (2022) 134236.
[64] Y. Li, H. Chen, L. Chen, et al., Appl. Catal. B 318 (2022) 121779.
[65] W. Chen, S. Yang, H. Liu, et al., Environ. Sci. Technol. 56 (2022) 10442–10453.
[66] Z. Wang, J. Lan, M. Haneda, et al., Catal. Today 376 (2021) 222–228.
[67] S. Liu, P. Yao, Q. Lin, et al., Catal. Today 382 (2021) 34–41.
[68] J. Wan, J. Chen, R. Zhao, et al., J. Environ. Sci. China 100 (2021) 306–316.
[69] X. Wei, Q. Ke, H. Cheng, et al., Chem. Eng. J. 391 (2020) 123491.
[70] W. Zhao, K. Zhang, L. Wu, et al., J. Colloid Interface Sci. 581 (2021) 76–83.
[71] J. Cao, X. Yao, F. Yang, et al., Chin. J. Catal. 40 (2019) 95–104.
[72] W. Si, H. Liu, T. Yan, et al., Appl. Catal. B 269 (2020) 118797.
[73] I. Song, S. Youn, H. Lee, et al., Appl. Catal. B 210 (2017) 421–431.
[74] C. Sun, W. Chen, X. Jia, et al., Chin. J. Catal. 42 (2021) 417–430.
[75] J. Liu, H. Cheng, H. Zheng, et al., ACS Catal. 11 (2021) 14727–14739.
[76] F. Liu, W. Shan, Z. Lian, et al., Appl. Catal. B 230 (2018) 165–176.
[77] L. Han, M. Gao, C. Feng, et al., Environ. Sci. Technol. 53 (2019) 5946–5956.
[78] H. Kubota, T. Toyao, Z. Maeno, et al., ACS Catal. 11 (2021) 11180–11192.
[79] Y. Xi, N.A. Ottinger, C.J. Keturakis, et al., Appl. Catal. B 294 (2021) 120245.
[80] K.A. Tarach, M. Jabłońska, K. Pyra, et al., Appl. Catal. B 284 (2021) 119752.
[81] Z. Gao, J. Pihl, T. LaClair, et al., Chem. Eng. J. 406 (2021) 127120.
[82] F. Gramigni, N.D. Nasello, N. Usberti, et al., ACS Catal. 11 (2021) 4821–4831.
[83] J. Liang, J. Tao, Y. Mi, et al., Chem. Eng. J. 409 (2021) 128238.
[84] Y. Sun, Y. Fu, Y. Shan, et al., Environ. Sci. Technol. 56 (2022) 17946–17954.
[85] R. Daya, D. Trandal, U. Menon, et al., ACS Catal. 12 (2022) 6418–6433.
[86] H. Wang, J. Jia, S. Liu, et al., Environ. Sci. Technol. 55 (2021) 5422–5434.
[87] S. Zhang, S. Ming, L. Guo, et al., J. Hazard. Mater. 414 (2021) 125543.
[88] Y. Ma, S. Cheng, X. Wu, et al., J. Catal. 405 (2022) 199–211.
[89] Y. Shi, J. Pu, L. Gao, et al., Chem. Eng. J. 403 (2021) 126394.
[90] H. Liu, C. You, H. Wang, ACS Catal. 11 (2021) 1189–1201.
[91] J. Zhang, P. Ji, L. Ren, et al., Chem. Eng. J. 444 (2022) 136657.
[92] R.G. Chitac, J. Bradley, N.D. McNamara, et al., Chem. Mater. 33 (2021) 5242–5256.
[93] H. Liu, C. Sun, Z. Fan, et al., Catal. Sci. Technol. 9 (2019) 3554–3567.
[94] H. Liu, Z. Fan, C. Sun, et al., Appl. Catal. B 244 (2019) 671–683.
[95] L. Li, P. Li, W. Tan, et al., Chin. J. Catal. 41 (2020) 364–373.
[96] C. Liu, L. Chen, J. Li, et al., Environ. Sci. Technol. 46 (2012) 6182–6189.
[97] X. Tang, Y. Shi, F. Gao, et al., Chem. Eng. J. 398 (2020) 125619.
[98] F. Wang, B. Shen, S. Zhu, et al., Fuel 249 (2019) 54–60.
[99] L. Kang, L. Han, P. Wang, et al., Environ. Sci. Technol. 54 (2020) 14066–14075.
[100] W. Tan, A. Liu, S. Xie, et al., Environ. Sci. Technol. 55 (2021) 4017–4026.
[101] R. Chen, X. Fang, J. Li, et al., Chem. Eng. J. 452 (2023) 139207.
[102] Y. Jae Park, D. Ho Kim, J.H. Lee, et al., Appl. Surf. Sci. 614 (2023) 156072.
[103] X. Qi, L. Han, J. Deng, et al., Environ. Sci. Technol. 56 (2022) 5840–5848.
[104] X. Fang, Y. Liu, Y. Cheng, et al., ACS Catal. 11 (2021) 4125–4135.
[105] X. Hu, J. Chen, W. Qu, et al., Environ. Sci. Technol. 55 (2021) 5435–5441.
[106] B. Wang, M. Wang, L. Han, et al., ACS Catal. 10 (2020) 9034–9045.
[107] R. Purbia, S.Y. Choi, H.J. Kim, et al., Chem. Eng. J. 437 (2022) 135427.
[108] Z. Chen, S. Ren, M. Wang, et al., Fuel 321 (2022) 124113.
[109] X. Li, Y. Niu, J. Li, et al., Chem. Eng. J. 454 (2023) 140180.
[110] Z. Xu, S. Impeng, X. Jia, et al., Environ. Sci. Nano 9 (2022) 2121–2133.
[111] Z. Wang, M. Jiao, Z. Chen, et al., Microporous Mesoporous Mater. 320 (2021) 111072.
[112] Y. Xu, P. Wang, Y. Pu, et al., Sep. Purif. Technol. 305 (2023) 122498.
[113] J. Yu, E. Zhang, L. Wang, et al., Energy Fuels 34 (2020) 2107–2116.
[114] Y. Chen, C. Li, J. Chen, et al., Environ. Sci. Technol. 52 (2018) 11796–11802.
[115] T. Tong, J. Chen, S. Xiong, et al., Catal. Sci. Technol. 9 (2019) 3779–3787.
[116] S. Guo, Z. Huang, L. Wang, et al., J. Hazard. Mater. 418 (2021) 126289.
[117] J. Chen, X. Fang, Z. Ren, et al., J. Mater. Chem. A 10 (2022) 6065–6072.
[118] I. Song, H. Lee, S.W. Jeon, et al., Nat. Commun. 12 (2021) 901.
[119] L. Yan, Y. Gu, L. Han, et al., ACS Appl. Mater. Interfaces 11 (2019) 11507–11517.
[120] Y. Xin, H. Li, N. Zhang, et al., ACS Catal. 8 (2018) 4937–4949.
[121] G. He, M. Gao, Y. Peng, et al., Environ. Sci. Technol. 55 (2021) 6995–7003.
[122] W. Wang, L. Wang, Y. Rao, et al., Appl. Surf. Sci. 618 (2023) 156638.
[123] Y. Shi, H. Yi, F. Gao, et al., J. Hazard. Mater. 413 (2021) 125361.
[124] H. Chang, X. Chen, J. Li, et al., Environ. Sci. Technol. 47 (2013) 5294–5301.
[125] R. Yang, S. Peng, B. Lan, et al., Small 17 (2021) e2102408.
[126] X. Zhang, X. Hu, S. Liu, et al., J. Environ. Chem. Eng. 10 (2022) 107318.
[127] Y. Geng, W. Shan, F. Liu, et al., J. Hazard. Mater. 405 (2021) 124223.
[128] W. Yoon, Y. Kim, G.J. Kim, et al., Chem. Eng. J. 434 (2022) 134676.
[129] Z. Liu, G. Sun, C. Chen, et al., ACS Catal. 10 (2020) 6803–6809.
[130] S. Xie, W. Tan, Y. Li, et al., ACS Catal. 12 (2022) 2441–2453.
[131] F. Wang, P. Wang, T. Lan, et al., ACS Catal. 12 (2022) 7622–7632.
[132] Q. Xu, Z. Fang, Y. Chen, et al., Environ. Sci. Technol. 54 (2020) 2530–2538.
[133] X. Shi, J. Guo, T. Shen, et al., Chem. Eng. J. 421 (2021) 129995.
[134] Y. Shi, H. Yi, F. Gao, et al., Sep. Purif. Technol. 265 (2021) 118517.
[135] C. Niu, B. Wang, Y. Xing, et al., J. Clean. Prod. 290 (2021) 125858.
[136] J. Song, S. Liu, Y. Ji, et al., Nano Res. 16 (2022) 299–308.
[137] S. Raja, M.S. Alphin, L. Sivachandiran, et al., Fuel 307 (2022) 121886.